

The 2003 Shell Event in η Carinae^{*}

Patricia A. Whitelock¹†, Michael W. Feast², Freddy Marang¹, Elmé Breedt³

¹ South African Astronomical Observatory, P.O.Box 9, 7935 Observatory, South Africa.

² Astronomy Department, University of Cape Town, 7701 Rondebosch, South Africa.

³ National Astrophysics and Space Science Programme, University of Cape Town, 7701 Rondebosch, South Africa.

Received date; accepted date

ABSTRACT

Near-infrared, *JHKL*, photometry of η Car is reported covering the period 2000 to 2004. This includes the 2003 shell event which was the subject of an international multi-wavelength campaign. The fading that accompanied this event was similar to, although slightly deeper than, that which accompanied the previous one. The period between these events is 2023 ± 3 days and they are strictly periodic. Their cause, as well as that of the quasi-periodic variations and secular brightening are discussed. It seems possible that all three types of variability are consequences of the binary nature of the star.

Key words: stars: individual: η Carinae - stars: variable: other - dust, extinction - infrared: stars.

1 INTRODUCTION

η Carinae is one of the most luminous stars in the Galaxy, and despite being one of the best studied objects in the sky¹, it remains poorly understood. While most of its luminosity is emitted in the mid-infrared, there is flux from and variability at all wavelengths from hard X-rays to radio. η Car is in some senses the archetypal astronomical object - which can only be fully characterized through observations across the entire electromagnetic spectrum. Davidson & Humphreys (1997) provide an extensive review of η Car, though there have been many developments since its completion².

It seems likely that we will soon be observing the details of similar objects in distant galaxies, so an understanding of this object potentially bears on many other topics.

Damineli (1996) discovered periodic variations in the equivalent width of He I 1.083 μ m, and in the visibility of high excitation lines, which correlated with *JHK* flux variations. He consequently suggested that η Car was in fact a binary system with an orbital period of about 5.5 years. Damineli predicted the next “shell phase” for 1997/98 and η Car was subjected to a period of intensified observations at all wavelengths (Morse et al. 1999). Not only did the “shell phase” occur on schedule, but it was accompanied by a number of unexpected phenomena, the most dramatic of which was a

very sharply defined X-ray minimum (Corcoran et al. 2001). This was associated with, among other things, a very clear dip in the *JHKL* light curves (Whitelock & Laney 1999), which we refer to as the “eclipse-like event” or simply the “event” in the following. Subsequent detailed examination of historical spectra (Feast et al. 2001) and monitoring at various wavelengths (e.g. 3 cm flux - Duncan & White 2003) established that a number of phenomena varied on this same timescale of 5.5 years.

The 5.5-year periodicity is now well established and most observers are convinced that η Car is a binary system. Some doubts do remain on the binary issue because, to date, none of the orbital parameter determinations have been convincing and there seem to be more questions about the underlying source(s) than ever before. The most recent “shell phase” occurred during 2003 and was observed even more intensively than the previous one. This paper is our contribution to the understanding of that event and we report broad-band near-infrared *JHKL* photometry obtained over the last 5 years. It continues the series of papers which collectively cover 32 years of photometry of η Car (Whitelock et al. 1983 & 1994; Feast et al. 2001 - henceforth Papers I, II and III). We start with a detailed discussion in section 3 of the source of the near-infrared flux as it is somewhat different from that of the visible, mid-infrared or far-infrared radiation. It is crucial that we have some clarity on this before we go on to consider the variations in the *JHKL* light curves and their various time scales in section 4.

In discussing the 5.5-year periodic phenomena, of which the 2003 shell event is the latest example, we refer our timings to the X-ray minimum observed by Corcoran et al.

^{*} This paper is based on observations made at the South African Astronomical Observatory.

† e-mail: paw@saa0.ac.za

¹ As of February 2004 NASA’s ADS lists 844 publications mentioning η Car in the abstract, 250 of them published since 2000.0.

² see, e.g., <http://etacar.umn.edu>.

(2001) and Corcoran (2004). In particular we use Julian Day 2452819.7 (2003.49) as phase zero; this coincides with the start of the minimum (the faintest point) of the X-ray “eclipse”. In doing this we make no particular comment on the correctness or otherwise of the Corcoran et al. model which has periastron at phase zero. The 2022 day period derived by Corcoran et al. is essentially identical to the 2023 days we derive from the *JHKL* light curves (section 4.2).

In Paper III we interpreted the dip in the infrared light-curve, which repeats every 5.5 yrs, as an eclipse of a hot spot. We now believe that the balance of evidence does not favour what would normally be called an eclipse, as is discussed below in detail. Nevertheless, we continue to use terminology that is usually associated with eclipses (e.g. “fourth contact” in the caption to Fig. 5) simply because it provides a succinct description of what we observe. It is important that the reader is clear that the use of this terminology does not imply the existence of eclipses.

This may well be the last paper in this series as we anticipate the closure of the infrared photometer on the 0.75m telescope at Sutherland within the next year.

2 INFRARED PHOTOMETRY

Monitoring of η Car in *JHKL* at SAAO in the period 1972-2000 established a quasi-cyclical variation with a period of the order of 5 years superposed on a secular increase in brightness (see Papers II and III). Table 1 contains the results of a continuation of this series of observations for the period 2000-2004. As in all recent work in this series, the observations were made with the SAAO MkII photometer on the 0.75m reflector at SAAO, Sutherland, using a 36 arcsec diaphragm encompassing the entire bipolar nebula (the Homunculus nebula). The individual results are accurate to better than ± 0.03 mag in *JHK* and ± 0.05 mag in *L*. The magnitudes are in the system defined by the standard stars of Carter (1990).

The magnitudes reported here, together with those reported in Papers I to III, are shown in Fig. 1 as a function of time. The last two cycles are shown on an expanded time scale in Fig. 2. Fig. 3 illustrates how the *J – L* colour of η Car changes as a function of time, while Fig. 4 shows a two-colour diagram with the various cycles identified by different symbols. There is a progression with time from the top right to the bottom left as the star gets bluer in all colours. The very first cycle has a lower *J – K* than might have been predicted from its *K – L* and the later colours. A brightening or ‘flare’ at *J* is seen during the second cycle, more specifically during the first few months of 1977. This could have been caused by a strengthening of the emission lines and the most likely culprit would be HeI 1.083 μm (see Whitelock (1985) for an indication of how this line affects the SAAO *J* magnitudes).

The near-infrared spectrum has been discussed by various authors (Paper I; Allen, Jones & Hyland 1985; McGregor, Hyland & Hillier 1988; Hamann et al. 1994; Smith 2002). The nature of the near-infrared emission is examined in detail below.

Table 1. Near-Infrared Photometry

JD –2450000	<i>J</i>	<i>H</i>	<i>K</i> (mag)	<i>L</i>
1709.00	2.490	1.599	0.454	–1.708
1712.22	2.487	1.597	0.450	–1.696
1714.25	2.474	1.598	0.449	–1.702
1737.23	2.499	1.615	0.466	–1.685
1738.21	2.507	1.619	0.463	–1.694
1743.21	2.514	1.607	0.458	–1.681
1808.66	2.543	1.643	0.479	
1834.63	2.551	1.627	0.473	–1.668
1858.61	2.543	1.651	0.480	–1.725
1862.61	2.547	1.643	0.483	–1.692
1869.62	2.508	1.619	0.470	–1.723
1881.61	2.533	1.620	0.453	–1.705
1890.62	2.518	1.614	0.448	–1.730
1926.56	2.572	1.672	0.498	–1.740
1929.54	2.574	1.683	0.504	–1.717
1962.47	2.571	1.664	0.495	–1.687
1965.45	2.559	1.670	0.489	–1.734
1976.45	2.580	1.666	0.481	–1.710
2032.34	2.487	1.586	0.448	–1.758
2037.29	2.479	1.591	0.438	–1.773
2068.24	2.462	1.560	0.418	–1.717
2087.24	2.476	1.571	0.422	–1.732
2093.25	2.492	1.577	0.428	–1.715
2116.19	2.440	1.531	0.384	–1.759
2211.62	2.454	1.538	0.393	–1.729
2239.61	2.422	1.525	0.409	–1.733
2257.60	2.407	1.518	0.384	–1.767
2261.62	2.454	1.534	0.390	–1.716
2267.62	2.394	1.529	0.391	–1.783
2283.58	2.426	1.512	0.371	–1.750
2284.61	2.464	1.551	0.405	–1.710
2285.58	2.456	1.551	0.410	–1.727
2287.57	2.456	1.547	0.411	–1.751
2288.59	2.489	1.586	0.466	–1.693
2289.64	2.466	1.562	0.426	–1.725
2318.52	2.468	1.568	0.419	–1.738
2320.49	2.430	1.538	0.399	–1.752
2324.49	2.462	1.575	0.427	–1.760
2346.43	2.474	1.555	0.415	–1.747
2350.43	2.464	1.558	0.411	–1.759
2352.40	2.452	1.551	0.402	–1.776
2381.37	2.451	1.549	0.409	–1.737
2386.33	2.461	1.553	0.411	–1.744
2421.25	2.469	1.544	0.406	–1.705
2426.23	2.463	1.553	0.408	–1.731
2428.27	2.472	1.558	0.412	–1.715
2451.26	2.460	1.539	0.406	–1.702
2455.24	2.467	1.550	0.406	–1.726
2486.23	2.514	1.585	0.427	–1.691
2490.19	2.512	1.582	0.420	–1.695
2492.20	2.513	1.587	0.421	–1.692
2525.68	2.487	1.561	0.397	–1.711
2529.67	2.512	1.580	0.413	
2534.65	2.495	1.591	0.431	–1.717
2563.64	2.533	1.577	0.420	
2564.63	2.488	1.585	0.419	–1.725
2568.64	2.478	1.557	0.399	–1.747
2573.63	2.473	1.566	0.412	–1.744
2593.62	2.490	1.563	0.413	–1.752
2603.60	2.479	1.562	0.411	–1.737

JD -2450000	<i>J</i>	<i>H</i>	<i>K</i>	<i>L</i>
	(mag)			
2661.57	2.490	1.554	0.382	-1.761
2664.57	2.485	1.560	0.387	-1.783
2665.59	2.481	1.550	0.394	-1.770
2667.56	2.480	1.554	0.390	-1.781
2675.56	2.483	1.557	0.393	-1.761
2676.51	2.483	1.562	0.386	-1.783
2680.52	2.512	1.560	0.377	-1.747
2689.49	2.481	1.561	0.404	-1.760
2690.44	2.497	1.548	0.399	-1.749
2691.49	2.499	1.563	0.399	-1.755
2692.48	2.483	1.552	0.390	-1.745
2693.52	2.482	1.553	0.389	-1.759
2694.50	2.487	1.551	0.385	-1.746
2695.48	2.484	1.553	0.396	-1.757
2696.55	2.477	1.554	0.396	-1.749
2697.54	2.474	1.555	0.391	-1.752
2698.50	2.503	1.548	0.384	-1.723
2699.47	2.478	1.547	0.388	-1.757
2700.45	2.504	1.546	0.381	-1.719
2701.52	2.481	1.539	0.389	-1.751
2702.46	2.489	1.542	0.384	-1.727
2710.44	2.476	1.556	0.383	-1.747
2711.49	2.477	1.540	0.378	-1.756
2712.54	2.462	1.529	0.368	-1.757
2715.53	2.488	1.529	0.327	-1.784
2716.43	2.455	1.511	0.359	-1.785
2752.34	2.426	1.454	0.298	-1.806
2753.33	2.428	1.458	0.300	-1.793
2754.31	2.402	1.452	0.294	-1.806
2755.32	2.406	1.448	0.298	-1.807
2756.30	2.406	1.434	0.290	-1.806
2758.31	2.376	1.429	0.278	-1.830
2759.36	2.399	1.423	0.282	-1.816
2760.29	2.397	1.436	0.280	
2761.29	2.384	1.424	0.282	-1.806
2762.29	2.396	1.428	0.283	-1.814
2764.42	2.382	1.430	0.273	-1.809
2773.39	2.355	1.400	0.270	-1.825
2774.26	2.324	1.392	0.256	-1.842
2775.28	2.344	1.392	0.257	-1.850
2777.23	2.337	1.386	0.256	-1.840
2778.27	2.339	1.389	0.255	-1.837
2779.25	2.335	1.388	0.254	-1.856
2794.24	2.339	1.360	0.240	-1.812
2795.21	2.339	1.367	0.239	-1.826
2797.22	2.327	1.351	0.237	-1.820
2798.22	2.326	1.346	0.225	-1.807
2800.22	2.324	1.349	0.227	-1.824
2801.20	2.321	1.332	0.214	-1.810
2802.23	2.305	1.317	0.209	-1.817
2803.23	2.311	1.338	0.222	-1.827
2804.21	2.299	1.315	0.217	-1.833
2805.21	2.293	1.319	0.211	-1.831
2806.20	2.305	1.318	0.211	-1.821
2807.20	2.292	1.307	0.208	-1.829
2809.28	2.291	1.310	0.207	-1.843
2810.27	2.291	1.301	0.200	-1.815
2811.26	2.282	1.301	0.203	-1.836
2813.30	2.283	1.308	0.221	-1.800
2814.29	2.281	1.307	0.215	-1.813

Table 1. continued

JD -2450000	<i>J</i>	<i>H</i>	<i>K</i>	<i>L</i>
	(mag)			
2815.22	2.287	1.312	0.217	-1.785
2816.33	2.267	1.318	0.238	-1.785
2817.25	2.289	1.318	0.239	-1.773
2818.19	2.301	1.324	0.244	-1.756
2819.27	2.300	1.328	0.249	-1.748
2820.21	2.288	1.325	0.261	-1.728
2821.26	2.307	1.340	0.274	-1.726
2823.23	2.303	1.352	0.297	-1.713
2825.19	2.332	1.384	0.324	-1.695
2826.16	2.349	1.400	0.333	-1.669
2828.25	2.366	1.424	0.370	-1.663
2831.21	2.403	1.450	0.400	-1.581
2832.20	2.407	1.459	0.406	-1.597
2833.21	2.414	1.472	0.413	-1.558
2834.21	2.413	1.484	0.425	-1.572
2835.19	2.420	1.485	0.430	-1.585
2840.25	2.436	1.487	0.449	-1.582
2841.25	2.440	1.484	0.441	-1.560
2842.21	2.421	1.474	0.437	-1.569
2843.20	2.429	1.473	0.436	-1.586
2844.20	2.423	1.469	0.437	-1.560
2845.20	2.408	1.451	0.418	-1.562
2846.19	2.406	1.459	0.433	-1.561
2847.19	2.412	1.449	0.416	-1.561
2848.19	2.399	1.438	0.407	-1.570
2849.19	2.394	1.436	0.395	-1.559
2850.19	2.363	1.431	0.398	-1.585
2852.19	2.346	1.413	0.379	-1.625
2854.19	2.354	1.411	0.384	-1.595
2855.19	2.341	1.402	0.367	-1.617
2856.19	2.311	1.391	0.358	-1.645
2857.19	2.353	1.394	0.363	-1.610
2858.22	2.329	1.385	0.356	-1.626
2865.19	2.300	1.369	0.342	-1.653
2868.19	2.303	1.378	0.335	-1.652
2869.19	2.302	1.375	0.330	-1.671
2886.23	2.268	1.322	0.283	-1.697
2887.24	2.261	1.331	0.286	-1.703
2891.23	2.246	1.320	0.278	-1.720
2893.23	2.256	1.300	0.270	-1.729
2894.22	2.261	1.326	0.269	-1.704
2896.23	2.232	1.333	0.274	-1.767
2918.64	2.240	1.319	0.272	-1.721
2931.64	2.238	1.322	0.260	-1.696
2932.63	2.252	1.329	0.265	-1.691
2933.64	2.244	1.336	0.274	-1.731
2955.62	2.265	1.351	0.298	-1.727
2959.62	2.255	1.358	0.301	-1.744
2961.61	2.271	1.362	0.294	-1.718
2969.61	2.264	1.359	0.290	-1.723
2971.60	2.247	1.370	0.292	-1.728
2972.61	2.269	1.365	0.305	-1.705
2973.61	2.261	1.371	0.285	-1.714
2974.61	2.266	1.386	0.290	-1.716
2975.61	2.250	1.351	0.286	-1.726
2978.62	2.269	1.367	0.312	-1.756
3026.50	2.287	1.434	0.352	-1.738
3029.60	2.300	1.435	0.357	-1.731
3030.50	2.311	1.435	0.361	-1.680

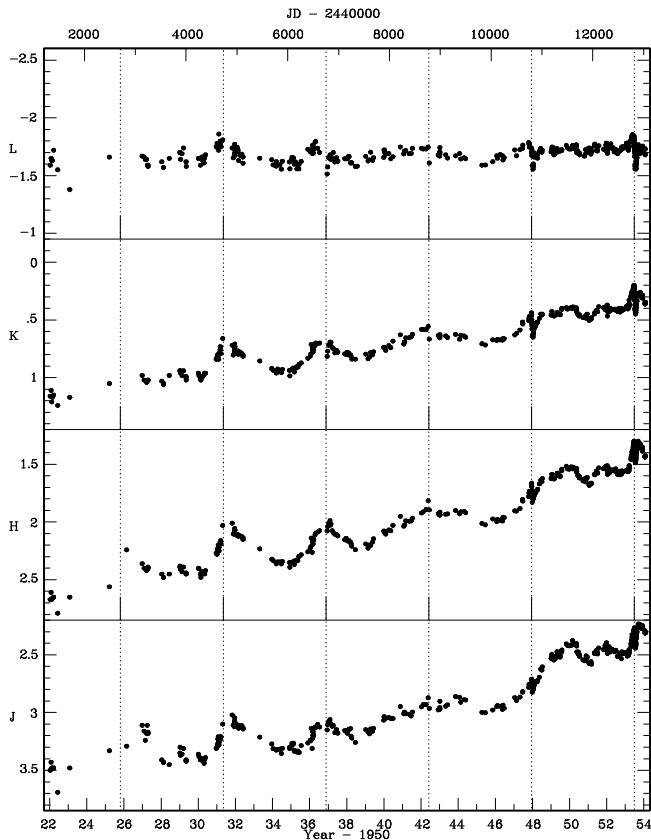


Figure 1. The *JHKL* magnitudes for η Car over the last 32 years. The dotted lines mark the positions of phase zero calculated according to the X-ray ephemeris (see section 1).

3 ORIGIN OF NEAR-INFRARED FLUX

Most of the flux from η Car, famously, emerges at mid- to far-infrared wavelengths and comes from dust in the Homunculus emitting over a range of temperatures (e.g. Smith et al. 2003 and references therein). This thermal emission is presumed to be reprocessed short-wavelength radiation from the central star(s). At radio (cm) wavelengths we see optically thick free-free emission from the stellar wind and from gas ionized by the central source(s) (e.g. White et al. 1994), while in the visual we see mostly scattered light from the Homunculus except at very high spatial resolution near the centre of the nebula, where the reddened stellar wind can be resolved (Morse et al. 1998). The emission line contribution to visual magnitudes is important, but it seems to originate at some remove from the main continuum source, in the outer parts of the stellar wind.

The near-infrared continuum has been attributed variously to scattered light, free-free emission, hot dust and/or the optically thick extended stellar atmosphere of the central source. The difficulty in settling this lies, at least partially, with the patchy, variable and uncertain level of the circumstellar extinction (see section 4.1).

While images of η Car are extended at all wavelengths they reach a minimum size, or a maximum central concentration, in the near-infrared at around $2\mu\text{m}$ (Allen 1989). This is an optical depth effect; at shorter wavelengths our line of sight does not penetrate far into the dust and at longer wavelengths emission from that dust dominates what we observe.

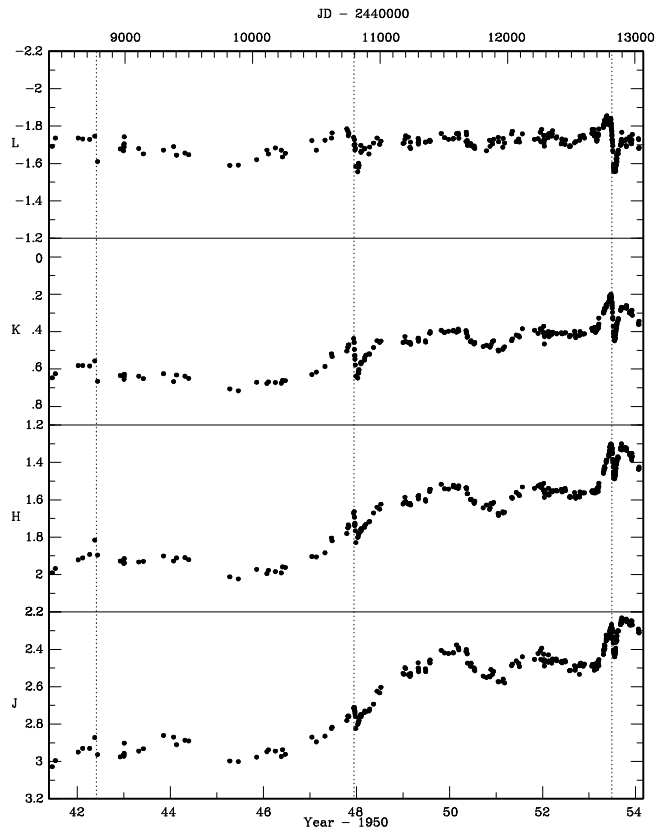


Figure 2. As for Fig. 1, but showing only the last two cycles.

Smith & Gehrz (2000) have conjectured, on the basis of morphological changes, that most of the near-infrared radiation does not come directly from the star itself, but from variably illuminated circumstellar ejecta. It is clear from their images that there is low level continuum emission scattered from the dust in the Homunculus in the same way as the optical light is scattered.

In a detailed analysis of 2 to $12\mu\text{m}$ images Smith, Gehrz & Krautter (1998) estimate the $2\mu\text{m}$ contribution scattered from the bipolar lobes as 13.4 percent. Walsh & Ageorges (2000), on the basis of *JHK* polarization measurements and the similarity of the polarization morphology to that observed in visual bands, also argue that scattering dominates everywhere except in the central core. However, they find less polarization at *JHK* than they expect from an extrapolation of the polarization at shorter wavelengths and suggest that this might be due to dilution by non-polarized emission. They consider dilution of the scattered light by hot dust emission, but reject it because the effect would be much stronger at *K* than at *J*, contrary to what is observed. Dilution by free-free emission would not be strongly wavelength dependent and we suggest that emission of this kind is a significant contributor, as is discussed below.

A small component of the flux (< 10 percent of the total at *K*) must come from direct line emission (Smith & Gehrz 2000), including a small contribution from the narrow emission lines in the Weigelt blobs (these are bright knots in the ejecta $< 0''.3$ from the central star (Smith 2002)). Lines such as $\text{Br}\gamma$ are strongly concentrated towards the core regions and presumably originate in the extended stellar

wind and surrounding HII region, or just inside the dusty torus (e.g. Smith et al. 1998; Smith & Gehrz 2000).

Van Boekel et al. (2003) estimate that in early 2002 about 200 Jy, or almost half the $2.39 \mu\text{m}$ flux, came from a volume with a diameter of 5 mas or 11 AU (at a distance of 2.3 kpc). This would imply a minimum blackbody temperature of 2300K (assuming no extinction); the temperature would be higher if allowance were made for plausible extinction. They conclude that they have spatially resolved the ionized stellar wind. It is clear from their fig. 1 image (taken on 2 February 2002, van Boekel private communication) that the rest of the flux in their 1.4 arcsec diameter image, comes from the immediate circumstellar environment, including the Weigelt blobs, and from the polar wind extensions to the NW and SE.

It is interesting to compare the image from van Boekel et al. (2003) (which is actually clearer in the reproduction by Richichi & Paresce 2003) with those at similar wavelengths discussed by Smith et al. (1998) and Smith & Gehrz (2000), noting that some time-dependent morphological changes must be expected. In the small area covered by the van Boekel et al. image one does not see the structure to the NE or SW and therefore has no sense of the equatorial “torus” which is prominent at longer wavelengths (Smith et al. 1998). It is not clear if this “torus” is a low resolution optical illusion or if it is real and variable (see also Smith et al. 2002). However, the similarity of the structure seen in fig 4a of Smith et al. (1998) - a deconvolved $2.16 \mu\text{m}$ image to which $\text{Br}\gamma$ must be a significant contributor - and the radio images from Duncan & White (2003) at certain phases, suggests that variable free-free emission is a real feature of the gas in this region (see below).

It is not clear whether we need to postulate the existence of any significant quantities of hot ($T \gg 400\text{K}$) dust in η Car. If there is dust at $T \sim 1000\text{K}$ then it would have a much greater influence at L than at shorter wavelengths and the fact that the variability at L has rather different characteristics, both in terms of secular changes and quasi-periodic variations, may indicate a dominant contribution from dust at this wavelength. Rigaut & Gehring (1995) concluded that colours derived from high spatial resolution images at $JHKL'M$ did indicate the presence of 1000K dust within 100 AU of the central star. Given the results of van Boekel et al. (2003), the very patchy extinction and the distribution of line emission, it is not clear that the colours can be interpreted in this way. Smith et al. (2003) require a dust component at 550K in the core to explain a fraction of the $4.8 \mu\text{m}$ flux, and their analysis would not rule out a small contribution from even hotter dust. The Smith et al. (2003) dust, at 550K, would contribute about 25 percent of the flux we observe at L .

It seems reasonably certain that free-free emission is a major contributor to the JHK flux, but it is difficult to establish exactly what proportion of the emission arises in this way. There is limited evidence for similar morphological changes in the 3 cm (Duncan & White 2003) and near-infrared images (Smith & Gehrz 2000), in the sense that the radio images are clearly most point-like around phase zero, and near-infrared images may show a similar tendency (see section 4.3). The fact that there is rather little correlation between the near-infrared quasi-periodic luminosity variations and the 3 cm emission (Duncan & White 2003;

White 2004) (K and 3 cm emission seem to have been anti-correlated between 1992 and 1998) must be attributed to optical depth effects, with the emitting regions being largely optically thick at 3 cm and partly optically thin at $2 \mu\text{m}$.

We can estimate from the 3 cm flux that there could plausibly be a very significant contribution at JHK , and possibly L , from free-free emission as follows: assuming the emission is partly optically thick, with a power law spectrum $S_\nu \propto \nu^\alpha$ and a spectral index, $\alpha = +0.6$ (for an unrealistic steady state, isothermal, radially symmetric wind (Wright & Barlow 1975)); the free-free flux at K and L would vary between 230 and 1060 Jy, when the 3 cm flux went from 0.7 to 3.2 Jy (1992 to 1998 Duncan & White 2003). The observed K flux ranges from 320 to 430 Jy and experiences an uncertain reddening, while that at L is about 1300 Jy. The predicted values will be greater if the power law is steeper, as it typically is for WR winds, or smaller if the emission has become optically thin at wavelengths longer than K . This serves only to illustrate that significant contributions from free-free are likely.

Using the information from van Boekel et al. (2003), Smith & Gehrz (2000) and Smith et al. (1998) we estimate that the flux at K measured through a large aperture (in late 1998) is made up very roughly as: 15 percent light scattered by cool dust, mostly in the Homunculus nebula, 5 percent from emission lines mostly close to the core, 30 percent in the equatorial “torus” (free-free), 30 percent in the unresolved core and 20 percent from the region within about 0.7 arcsec of the central core - some of this will be free-free emission from the polar outflow, but if there is hot dust present it will be within 0.7 arcsec of the central core and part of this component.

4 INFRARED VARIABILITY

The infrared light curves (Fig. 1) show variability on a variety of timescales that were discussed in Paper III. There is a secular brightening through all filters which is wavelength dependent, being most pronounced at J and barely discernible at L . There is the, now well established, “eclipse-like event”, with a period of 2023 days which is most evident in the L data - where it is deepest and not masked by other variations. Finally there are quasi-periodic variations which occur on roughly the same time scale as the events, but which do not seem to be strictly periodic. Despite the wealth of data none of these variations can be unambiguously explained. They are discussed below in more detail.

4.1 Secular Brightening

There is a very clear secular brightening of η Car in the $JHKL$ wavebands over the monitoring period of 32 years. Unfortunately our inability to properly characterize and model the periodic and quasi-periodic variations (discussed below), which are evident in all wavebands, also makes it impossible to describe these secular changes in detail.

While the changes at K could be consistent with a systematic linear brightening, it seems likely that at J η Car has been brightening faster over the last 15 than over the previous 15 years, and there can be no doubt that the overall change in colour has been greater over the last two cycles

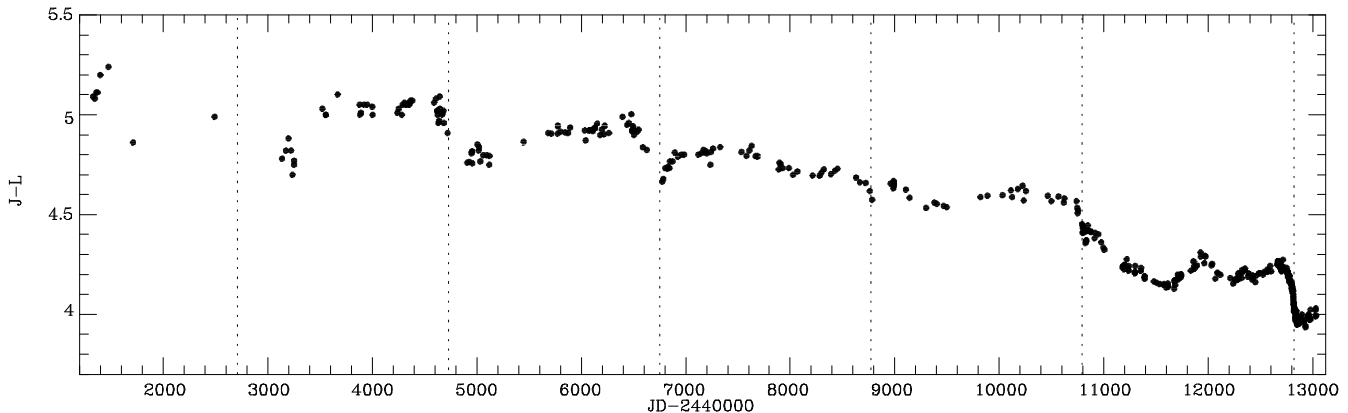


Figure 3. The $J - L$ colour as a function of Julian date. The dotted lines mark the epoch of the X-ray event, as in Figs. 1 and 2. Note the way the colour changes rapidly during the events and rarely returns afterwards.

Table 2. Linear rates of brightening.

band	rate mag.day ⁻¹	Δ mag 30 yrs
<i>J</i>	-11.2×10^{-5}	1.22
<i>H</i>	-10.8×10^{-5}	1.18
<i>K</i>	-7.0×10^{-5}	0.77
<i>L</i>	-8.6×10^{-6}	0.09

than previously. However, for the purpose of the discussion we treat all trends as linear and Table 2 lists the parameters derived from a simple least squares fit to the magnitudes as a function of Julian Date. The last column lists the magnitude change over 30 years. A comparison with the numbers in table 2 of Paper II suggests that the rate of brightening has increased significantly, particularly at *J* and *L*, but it is important to remember that the exact positions of the end points affect this simple line fitting. Removing the early points, which fall off the general trend of colour seen in Fig. 4, changes the values quoted in Table 2 by only a small amount.

Davidson et al. (1999) discuss an apparently increased rate of brightening at near-infrared and visual wavelengths during 1998. This was seen most dramatically in the HST/STIS observation of the central star (area $0''.1 \times 0''.15$) where the flux at 4000\AA increased by 0.83 mag in just over one year (see also section 4.3). Examining the infrared changes, in the context of Figs. 1 and 3, and the variations that have taken place in recent years, it is clear that there have been phases of rapid change; 1998 was one and so was 1981. Of course we have no idea what HST/STIS observations might have shown in 1981, but the changes of 1998 may be a common occurrence.

Various possible causes of the secular brightening were discussed in Paper II. It remains possible, with many caveats, that a reduction of the extinction due to dust or an increase in flux from the central source or a combination of the two may be affecting the changes. The secular brightening is accompanied by a change in the colours, as is illustrated in Figs. 3 and 4. It is evident from these two diagrams that the colour changes are more episodic than gradual and that the colours tend to change discontinuously

at the epochs of the event. This suggests that whatever happens at around these epochs may also be driving the secular brightening and it would not be consistent with a gradual thinning of the dust as the major cause of brightening at *JHK*.

It is difficult to prove that the secular brightening is directly related to the periodic events, but the magnitude changes illustrated in Figs. 1 and 2 also support that interpretation. At *L* there is very little secular change and the quasi-periodic variations always peak just before the eclipse-like event. At *J*, where the secular changes are at their largest the quasi-periodic variations very clearly peaked after the eclipse-like event in both 1998 and 2003/4. This difference is more marked at *J* than at *H* where the quasi-periodic variations had their largest amplitude at earlier epochs. Until we can disentangle the different sources of variability it will not be possible to prove or disprove the link between the secular changes and the eclipse-like events.

It is clear, from the high spatial resolution HST observations that the extinction towards the central regions is very patchy (Davidson et al. 1995). Furthermore, different components of the emission originate in spatially separate locations and may experience different extinctions. This applies to different spectral components at the same wavelength; the continuum, the broad lines and the narrow lines are produced in different places. Furthermore, maps at *J*, *K* and *L* show slightly different morphology, suggesting that we are seeing to different depths in the continuum at these different wavelengths (e.g. Rigaut & Gehring 1995). The reddening law for the circumstellar extinction in η Car is thought to be peculiar (Paper II; Davidson et al. 1995 and references therein; Walsh & Ageorges 2000), possibly because of an unusual size distribution of the dust grains. However, the patchy nature of the extinction combined with the spatial separation of the various emission components, actually make it very difficult to deduce the reddening law (Hillier & Allen 1992). Thus, while the magnitude changes listed in Table 2 are not what we would expect from the reduction of normal reddening we cannot rule out that explanation entirely.

Groh & Daminieli (2004) noted secular changes in the emission lines over the last 11 years, in addition to the variations that take place over the 2023 day period. They record

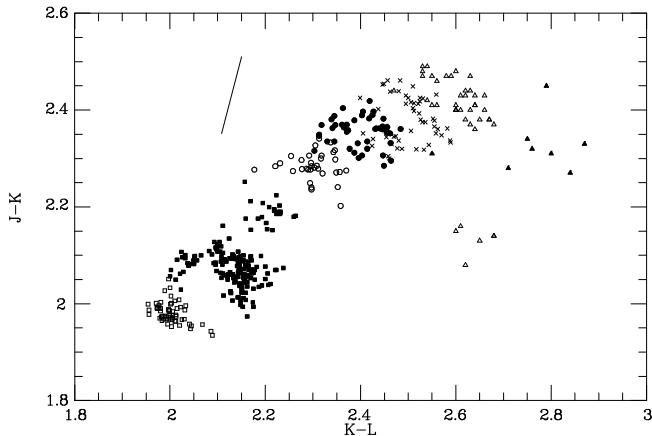


Figure 4. Two-colour diagram for η Car; different symbols show the various cycles as marked in Figs. 1 and 3, going from earliest to latest as follows: closed triangles, open triangles, crosses, closed circles, open circles, closed squares, open squares. The line shows the change in colours that would occur if the interstellar extinction were to alter by $A_V = 1$ mag (this assumes a normal reddening law which is probably not applicable to η Car; it is shown for illustrative purposes only).

a general weakening of the high- and intermediate-excitation lines. The equivalent width of the HeI $\lambda 6678$ emission has been gradually decreasing, while the absorption component of this P Cygni line has been getting deeper. These changes suggest that the optical depth of the emitting region(s) is gradually increasing and cannot be attributed to an expansion or thinning of the obscuring dust.

Although it is possible to envisage the colour changes, illustrated in Figs. 3 and 4, as the consequence of grain destruction by increased ultraviolet flux at around phase zero, the grains would have to be close to the central star. They would therefore be radiating at a high temperature and their destruction should have noticeably reduced the L flux. In fact, the secular change in L has been very small, it has been brightening by less than 0.1 mag in 30 year - so this explanation must be rejected.

4.2 The Eclipse-Like “Event”

First we estimate the interval between events. The 2003 minimum at K was on JD 2452840.3. In the previous cycle the minimum was between 2450809.6 and 2450824.6, but nearer the latter so we take it to have been on 2450817. The event in the cycle before was not usefully observed, although minimum must have been a few days after 2448783 (contrast J and L in Fig. 2 given that the decline starts sooner at L) and for the cycle before that it was at 2446775.6 or a few days before. These timings are consistent with the event being a precisely cyclical event and our best estimate for the period is 2023 ± 3 days. This is almost identical to the period determined from the X-ray events (Corcoran 2004) and not significantly different from the 2025 days determined from the spectroscopic changes (Groh & Daminieli 2004), or the 2022.1 ± 0.4 days that Daminieli et al. (in preparation) derive from a more detailed analysis.

Fig. 5 allows us to compare the 1998 and 2003 events and to make a comparison with the X-ray light curve (Corco-

Table 3. Comparison of eclipse-like events.

band	depth		2003/1997	
	1997	2003	max	min
J	10%	14%	1.49	1.43
H	15%	15%	1.39	1.38
K	18%	20%	1.24	1.20
L	19%	24%	1.06	1.00

ran 2004). The two events naturally separate in magnitude at JHK because of the long-term trend. At L , where the long-term trend is negligible over 5 years, the differences in shape and amplitude are minor. It is of course very difficult to be certain whether changes at any wavelength are linked to the event or to some other, possibly unrelated, variations. During the event the hard X-ray emission drops to one percent of the flux before minimum (Hamaguchi et al. 2003; Corcoran 2004) and stays close to that level for about 70 days. The infrared event is preceded by a brightening at all wavelengths (but see section 4.3), as is the X-ray event. In marked contrast to the X-ray light curve, the infrared event involves flux decreases of only 10 to 24 percent and is flat bottomed only at L and only for about 20 days. While the oscillations in the X-ray flux make it difficult to pinpoint the time of ingress, it is clearly earlier than it is at infrared wavelengths. Within the near-infrared light curves ingress starts earliest at L and latest at J where it more or less coincides with the well-defined start of X-ray minimum; the delay between L and J is about 7 days. The K minimum occurs at X-ray phase 0.011.

According to the data of Fernández Lajús et al. (2003) the fading at visual wavelengths, $BVRI$, started later still (JD 2452826 at V), about 10 days after J . It should be borne in mind that the $BVRI$ measurements are much more strongly influenced by scattered light from the Homunculus than are $JHKL$. The optical high-excitation emission lines disappear around phase zero (Groh & Daminieli 2004). Note that these originate in an extended region around the central star, not in the stellar wind itself (Smith et al. 2000).

The data in Table 3 allows us to compare the depths of the last two events. The second and third columns give the depth at minimum, expressed as a percentage of the flux just before the event. The next two columns are the flux ratio, 2003 divided by 1997/8, for the pre-event maximum (column 5) and the event minimum (column 6). The errors are about two percent on all the numbers. Taking these at face value we see that the event stayed the same or deepened slightly between 1997/98 and 2003. This means that whatever has brightened during that interval decreases in approximately the same proportion as or slightly more than before. Although it is clear that the event is about 10 percent deeper at L than at J , and of intermediate depth in the intervening wavebands, this may be a little deceptive. The time of peak brightness is wavelength dependent (possibly because of the secular trend) and J does not reach its peak until after the event, as in earlier cycles. Obviously the eclipse-like event would be deeper at J if we measured it with respect to this peak rather than to the maximum before the event.

The 1998 event showed a two step egress (Paper III, figs. 4 and 7), the shallow part of which extended in phase from about 0.01 to 0.09, ending at about the same time

as the low excitation phase of the emission lines. The 2003 event also shows a two phase egress, but the shallow part is brief, extending only from phase 0.01 to 0.036. That is, it ends about the same time as the X-ray event comes out of its minimum. It was clear from the historical analysis of Paper III that the low excitation event does not cover the identical phase every time, but we have almost no information about infrared flux levels for earlier events. It will be interesting to see if the 2003 return of the high excitation spectrum correlates with the infrared light curve in the same way as it did in the previous event.

Gull et al. (2003) describe changes in the ultraviolet as observed at high spatial and spectral resolution with HST/STIS during the critical phases. Visibility of the central source dropped, but not uniformly throughout the ultraviolet, so they suggest that the fading was caused by multiple line absorptions both in the source and in the intervening ejecta. High excitation lines diminished or disappeared while lines originating from lower levels strengthened. Observations with FUSE also show striking wavelength-dependent absorptions during the event (Iping et al. 2003). Longward of 1100Å the overall flux dropped by 10 to 30 percent, but shortward of this wavelength there were intervals with no decrease in flux at all. Thus dust absorption must play a negligible role in producing the events.

Martin et al. (2004) describe HST/STIS data relevant to the event which is particularly interesting as it isolates the behaviour of the central star. They find that H α fades at phase 0.95, much earlier than even the X-rays and at about the same time as the pre-event brightening starts at *JHKL*, but brightens again at phase 1.04. The continuum at 6770 Å brightens as H α fades. The *V* continuum does not show any event-related change at all, in obvious contrast with ground-based *V* observations which encompass the whole Homunculus.

4.3 Quasi-periodic Variations

In Paper II we noted quasi-periodic variations in the *JHKL* data for η Car covering 20 years up to 1994; their characteristic time scale was about 5 years. Marking the 2023 day cycles in Fig. 1 guides the eye to see the changes at this period. It is particularly clear in the *H* light curve that peaks occur at around the time of events at five of the six marked intervals. A Fourier analysis of these data, after removing the long-term trend (assumed to be linear), indicates primary periods of 1961 days at *L*, 2091 days at *K*, 2074 days at *H* and 2044 days at *J*. Given that the variations are not sinusoidal, and that there are other changes on different time scales, these results are consistent with an underlying period of 2023 days. However, we would probably not deduce strict periodicity for these particular variations if it were not for the 2023 day periodicity of the eclipse-like events.

The peak-to-peak amplitude in magnitudes of the quasi-periodic variations is 0.2 to 0.3 at *J*, 0.35 to 0.45 at *H*, 0.2 to 0.3 at *K* and 0.1 to 0.2 at *L*; the maximum amplitudes are good to ± 0.03 mag. It is at *L* that these variations are at their most repeatable (see Paper III), with the maximum always occurring just before the eclipse-like minimum. We might estimate that roughly one-third of the *L* flux originates from warm dust emission (see section 3). Subtracting this dust flux leaves a component with an amplitude of

about 0.3 mag - comparable to values measured at *J* and *K*. Unfortunately a meaningful comparison of the spectral energy distribution of these quasi-periodic variations cannot be made without removing the contributions from other sources of emission - which cannot be quantified as yet.

At *J*, *H* and *K* the peak that occurs just before the event minimum seems to form part of these quasi-periodic variations. Sometimes this peak is very close to the broad maximum, as in 1981 and 1986/7, at other times it is very early on, as in 1997/8. The most recent variations may have increased in amplitude at *J* relative to *H*, but it is difficult to be certain because of the poorly characterized secular changes.

Smith & Gehrz (2000) compare two high-spatial-resolution *K* measurements of η Car made in May 1995 (JD 2449852 \pm 15, phase 0.53) and on 6 September 1998 (JD 2451063, phase 0.13). They find that the flux within a central 1'' aperture increases by a factor of 1.93 between 1995 and 1998 and its distribution becomes more point-like in 1998 when it is brightest. The data in our Table 1 suggests that the integrated *K* flux goes up by a factor of 1.27 over the same period (note that Smith & Gehrz find that the integrated flux changes by only 13 percent from their images; the difference between their measurement and ours is only in the value from the 1998 NICMOS measurement). Davidson et al. (1999) discuss the brightening at other wavelengths (see also section 4.1) and note that the central star brightened in the optical and near-ultraviolet. The brightening seems to have been nearly wavelength independent.

van Genderen, de Groot & Sterken (2001) find luminosity peaks in the visual data following the same kind of pattern that we see in Fig. 1, although with amplitudes of only one or two tenths of a magnitude. They suggest that these may be a consequence of a binary companion triggering "S Doradus events", i.e. mass loss, from the primary and the mass moving into a disk or torus. They also discuss problematic aspects of this interpretation.

The radio flux also shows variability, by more than a factor of three, on this same time scale (Duncan & White 2003), although there does not seem to be much correlation between the intensities of the radio and near-infrared variations as was discussed in section 3. Duncan & White also interpret the changes as a consequence of the tidal transfer of material from the primary into a disk. The radio image is much more compact when the radio emission is faint - possibly it is only the extended component, with a diameter of 4 to 5 arcsec at maximum, that varies significantly and that it does so because of changing levels of ionizing radiation, as suggested by Duncan et al. (1995).

Damineli's (1996) discovery of the inverse correlation of the equivalent width of the He I 1.083 μ m line with the *H*-band flux led to a dramatic change in our thinking on η Car. Like many other aspects of the variability it is most easily understood as the consequence of changes in the optical depth of the emitting region(s).

It is vital that η Car be monitored at high spatial resolution in the near-infrared if further progress is to be made in interpreting the various changes and their relationship to the central star(s).

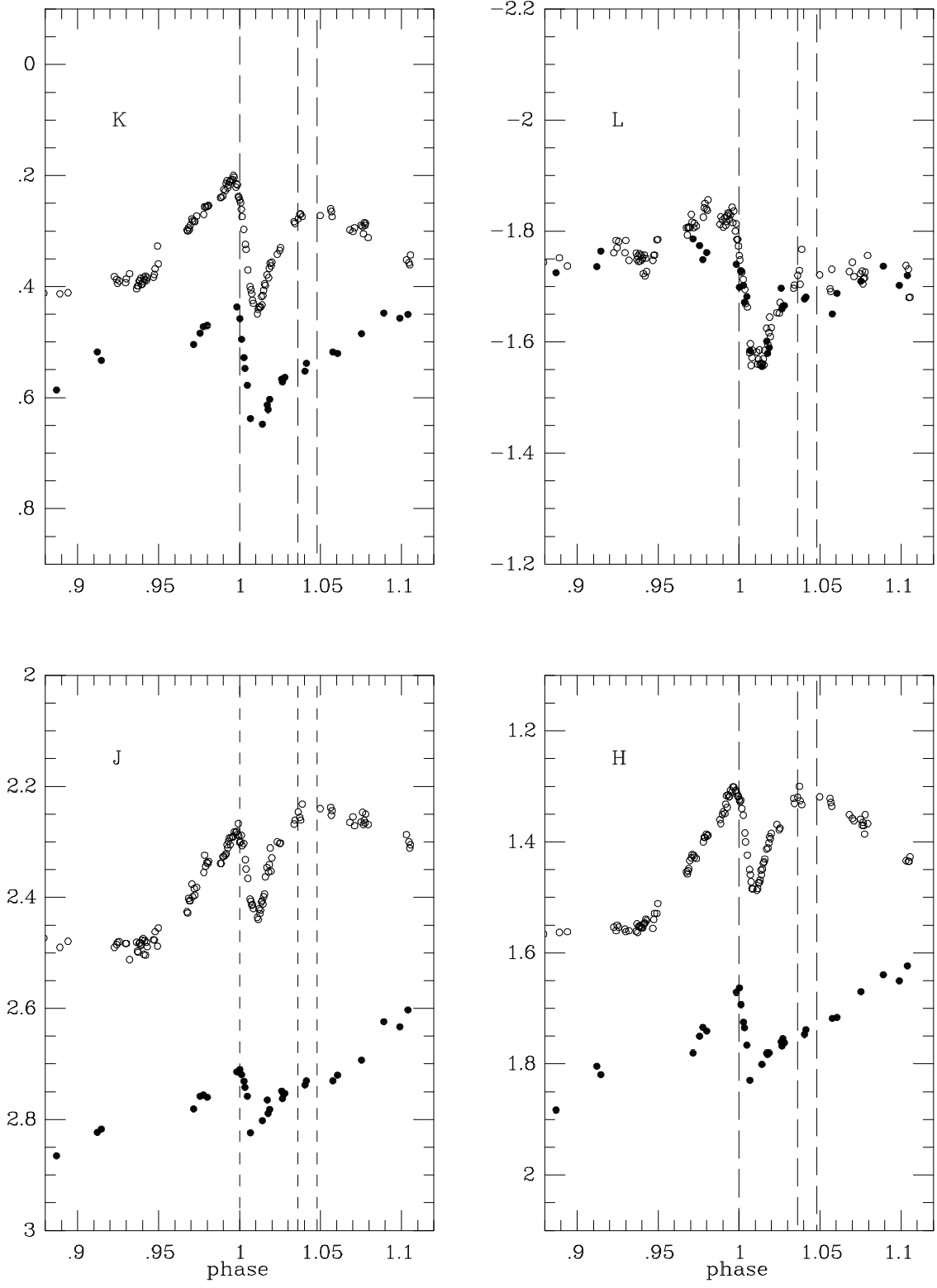


Figure 5. A comparison of the 1998 (solid symbols) and the 2003 (open symbols) events at the four wavelengths. The dashed lines are taken from the X-ray event (Corcoran 2004) and mark the phases of the start and end of X-ray minimum and fourth contact.

5 DISCUSSION

In view of the emphasis that Smith et al. (2000) put on the non-periodicity of the infrared flux variations (last paragraph of their section 4.2) it is important that we clarify this point. In section 4.2 we derived a period for the “eclipse-like events” of 2023 ± 3 days; this is, as far as current information allows us to determine it, a “precise period”. In contrast, the broad peaks seen in the *JHKL* light curves over the last 30 years (see section 4.3) are quasi-periodic.

The similarity of the timescale of the quasi-periodic variations and the period between events suggests that the underlying cause of these phenomena is the same and that they are both orbitally modulated variations. Furthermore, the secular variations are characterized by discontinuous colour changes which occur around phase zero in the 2023 day cycle, which suggests that they too may be driven by something associated with the orbital period.

The morphology of the X-ray light curve during the 1997/8 event was explained by Corcoran et al. (2001) in terms of a binary model with periastron passage at phase zero. The X-rays are produced by shock-waves in colliding stellar-winds and the specifics of the light curve can be reproduced if the mass-loss from η Car increases from $3 \times 10^{-4} M_{\odot} \text{yr}^{-1}$ by a factor of about 20 for a period of about 80 days following periastron. During the event the X-rays are absorbed in the dense wind resulting from the enhanced mass loss. Zanella et al. (1984) first suggested that the low-excitation spectroscopic phase and enhanced near-infrared emission might be caused by a shell ejection; although we note that they attributed the increased near-infrared flux to dust formation which is contrary to our results. When the 5.5 yr binary period started to look plausible various people conjectured that the close passage of the secondary in an elliptical orbit might trigger increased mass-loss at critical phases (e.g. Davidson 1999; Ishibashi et al. 1999).

Other evidence, cited in section 4.2, points to enhanced ultraviolet line opacity during the event, resulting in decreased excitation of emission lines at many wavelengths. Surprisingly there is no evidence for changes in the temperature or luminosity of the visual continuum from the central source and it is possible that the optical depth is sufficiently high that what is observed at high spectral resolution is well away from where the action is taking place. We have insufficient information to be certain what is causing the event observed at *JHKL*, but we might conjecture that free-free emission, coming from a rather broad volume around the central source, will greatly decrease if its source of ultraviolet excitation is quenched when the secondary is enveloped in the material pulled from the primary or from the passage of the secondary through dense pre-existing circumstellar material.

In this picture the quasi-periodic changes would be explained in a similar way to the radio variations (Duncan & White 2003) if the secondary star is largely responsible for ionizing the HII region surrounding η Car. Orbital modulation of the source of ionizing radiation as it moves in and out of the denser parts of the circumstellar disk will drive the quasi-periodic variations. Much of the nebula must be optically thick at radio wavelengths but not in the near-infrared.

Thus the secular variations may also be the consequence of enhanced free-free emission as the newly ejected mass

joins the material around η Car and emits at *JHK* wavelengths. It may well be possible to use the information from the multi-wavelength campaign to establish where the material is building-up. We might speculate that if conditions become suitable for dust formation in these ejecta then radiation pressure could cause the dust and gas to be expelled with great efficiency.

ACKNOWLEDGMENTS

We are very grateful to Lisa Crause and Dave Laney for making some of the *JHKL* measurements and to John Menzies for a critical reading of the manuscript. We also thank the following for their comments and suggestions on the preprint: Mike Corcoran, Augusto Damineli, Kris Davidson, Roberta Humphreys, John Martin and an anonymous referee.

REFERENCES

- Allen D.A., 1989, *MNRAS*, 241, 195
 Allen D.A., Jones T.J., Hyland A.R., 1985, *ApJ*, 291, 280
 Carter B.S., 1990, *MNRAS*, 242, 1
 Corcoran M.F., 2004, http://lheawww.gsfc.nasa.gov/users/corcoran/eta_car/etacar_rxte_lightcurve/
 Corcoran M.F., Ishibashi K., Swank J.H., Petre R., 2001, *ApJ*, 547, 1034
 Damineli A., 1996, *ApJ*, 460, L49
 Davidson K., 1999, in: *Eta Carinae at the Millenium*, (eds.) J.A. Morse, R.M., Humphreys & A. Damineli, *ASP Conf. Ser.*, 179, 304
 Davidson K., Humphreys R.M., 1997, *ARAA*, 35, 1
 Davidson K., Ebbets D., Weigelt G., Humphreys R.M., Hajian A.R., Walborn N.R., Rosa M., 1995, *AJ*, 109, 1784
 Davidson K., Gull T.R. Humphreys R.M., Ishibashi K., Whitelock P.A., Berdnikov L., McGregor P.J., Metcalfe T.S., Polomski E., Hamuy M., 1999, *AJ*, 118, 1777
 Duncan R.A., White S.M., Lim J., Nelson G.J., Drake S.A., 1995, *ApJ*, 441, L73
 Duncan R.A., White S.M., 2003, *MNRAS*, 338, 425
 Feast M.W., Whitelock P.A., Marang F., 2001, *MNRAS*, 322, 741, Paper III
 Fernández Lajús, E., et al., 2003, *IBVS*, 5477
 van Genderen AM., de Groot M., Sterken C., 2001, in: *P Cygni 2000; 400 Years of Progress*, (eds.) M. de Groot & C. Sterken, *ASP Conf. Ser.* 233, 59
 Groh J.H., Damineli A., 2004, *IBVS*, 5492
 Gull T.R., Nielsen K.E., Vieira G.L. Hillier D.J., Walborn N., Davidson K., HST Treasury Team, 2003, *AAS*, 203, 5810
 Hamaguchi K., Corcoran M.F., White N.E., Damineli A., Davidson K., Gull T.R., 2003, *AAS*, 203, 5801
 Hamann F., Depoy D.L., Johansson S., Elias J., 1994, *ApJ*, 422, 626
 Hillier D.J., Allen D.A., 1992, *A&A*, 262, 153
 Iping R.C., Gull T.R., Sonneborn G., Massa D., Vieira G.L., Nielsen K.E., 2003, *AAS*, 203, 5808
 Ishibashi K., Corcoran M.F., Davidson K., Drake S.A., Swank J.H., Petre R., 1999, in: *Eta Carinae at the Millenium*, (eds.) J.A. Morse, R.M., Humphreys & A. Damineli, *ASP Conf. Ser.*, 179, 266
 Martin J.C., Koppelman M.D., HST Treasury Team, 2004, *AJ*, in press
 McGregor P.J., Hyland A.R., Hillier D.J., 1988, *ApJ*, 324, 1071

- Morse J.A., Davidson K., Bally J., Ebbets D., Balick B., Frank A., 1998, *ApJ*, 116, 2443
- Morse J.A., Humphreys R.M., Damineli A. 1999, *Eta Carinae at the Millennium*, ASP Conf. Ser. 179
- Richichi A., Paresce F., 2003, *The Messenger*, No. 114, 26
- Rigaut F., Gehring G., 1995, *Rev. Mex. A.A.*, 2, 27
- Smith N., 2002, *MNRAS*, 337, 1252
- Smith N., Gehrz R.D., 2000, *ApJ*, 529, L99
- Smith N., Gehrz R.D., Krautter, J., 1998, *AJ*, 116, 1332
- Smith N., Morse J., Davidson K., Humphreys R., 2000, *ApJ*, 120, 920
- Smith N., Gehrz R.D., Hinz P.M., Hoffman W.F., Mamajek E.E., Meyer M.R., Hora J.L., 2002, *ApJ*, 567, L77
- Smith N., Gehrz R.D., Hinz P.M., Hoffman W.F., Hora J.L. Mamajek E.E., Meyer M.R., 2003, *AJ*, 125, 1458
- van Boekel R., et al., 2003, *A&A*, 410, L37
- Walsh J.R., Ageorges N., 2000, *A&A*, 357, 255
- White S.M. et al., 1994, *ApJ*, 429, 380
- White S.M., 2004, http://www.astro.umd.edu/~white/images/eta_time_full.html
- Whitelock P.A., 1985, *MNRAS*, 213, 59
- Whitelock P.A., Feast M.W., Carter B.S., Roberts G., Glass I.S., 1983, *MNRAS*, 203, 385, Paper I
- Whitelock P.A., Feast M.W., Koen C., Roberts G., Carter B.S., 1994, *MNRAS*, 270, 364, Paper II
- Whitelock P.A., Laney C.D., 1999, in: J.A. Morse et al. (eds.) *Eta Carinae at the Millennium*, ASP Conf. Ser., 179, p. 258
- Wright A.E., Barlow M.J., 1975, *MNRAS*, 170, 41
- Zanella R., Wolf B., Stahl O., 1984, *A&A*, 137, 79